Published in final edited form as:
Biomech Model Mechanobiol. 2007 January ; 6(1-2): 63–72. doi:10.1007/s10237-006-0040-3.

CONVECTION AND DIFFUSION IN CHARGED HYDRATED SOFT TISSUES: A MIXTURE THEORY APPROACH

Hai Yao[1] and **Wei Yong Gu**[*]
Tissue Biomechanics Lab, Dept. of Biomedical Engineering, University of Miami, Coral Gables, FL

1*Dept. of Bioengineering, Clemson University, Clemson, SC*

Abstract

The extracellular matrix of cartilage is a charged porous fibrous material. Transport phenomena in such a medium are very complex. In this study, solute diffusive flux and convective flux in porous fibrous media were investigated using a continuum mixture theory approach. The intrinsic diffusion coefficient of solute in the mixture was defined and its relation to drag coefficients was presented. The effect of mechanical loading on solute diffusion in cartilage under unconfined compression with a frictionless boundary condition was analyzed numerically using the model developed. Both strain-dependent hydraulic permeability and diffusivity were considered. Analyses and results show that: (1) In porous media, the convective velocity for each solute phase is different. (2) The solute convection in tissue is governed by the relative convective velocity (i.e., relative to solid velocity). (3) Under the assumption that all the frictional interactions among solutes are negligible, the relative convective velocity for α-solute phase is equal to the relative solvent velocity multiplied by its convective coefficient (H^{α}) which is also known as the hindrance factor in the literature. The relationship between the convective coefficient and the relative diffusivity of solute is presented. (4) Solute concentration profile within the cartilage sample depends on the phase of dynamic compression.

Keywords

Biomechanics; Cartilage; Diffusion coefficient; Porous media; Transport

INTRODUCTION

Cartilage is an avascular tissue whose cells rely on the transport of molecules through its extracellular matrix (ECM) for nutrition. The ECM of cartilage primarily consists of water, collagen-proteoglycan network and ions (mostly, Na^+ and Cl^-). The ECM of cartilage can be treated as a charged porous fibrous material. Convection and diffusion are the major mechanisms for solute transport through the ECM(Grodzinsky 1983; Maroudas 1979; Mow et al. 1992; Maroudas 1975; Urban et al. 1978).

Investigation of solute transport in cartilaginous tissues is important for understanding mechano-biology of such tissues. Poor nutrition supply is believed to be one of the possible mechanisms for intervertebral disc (IVD) degeneration(Horner and Urban 2001). Numerous studies have been done on the solute transport in articular cartilage and IVD theoretically and experimentally. Recent studies in this area include experimental investigation of solute

*Corresponding author: W.Y. Gu, Ph.D. Department of Biomedical Engineering College of Engineering University of Miami P.O. Box 248294 Coral Gables, FL 33124-0621 USA Telephone: (305)284-5434 Fax: (305)284-4720 E-mail: E-mail: wgu@miami.edu.

transport in these tissues (Bonassar et al. 2000; Burstein et al. 1993; Garcia et al. 1996; Maroudas 1975; Torzilli et al. 1987; Urban et al. 1978; Leddy and Guilak 2003; O'Hara et al. 1990; Quinn et al. 2000; Quinn et al. 2001; Quinn et al. 2002; Nimer et al. 2003; Evans and Quinn 2005), theoretical analysis of solute transport in cartilaginous tissues and gels using mixture theories(Mauck et al. 2003; Yao and Gu 2004; Quinn et al. 2002; Levenston et al. 1997; Levenston et al. 1998; Levenston et al. 1999; Ferguson et al. 2004), and constitutive modeling of transport properties in these tissues(Gu et al. 2003; Gu et al. 2004; Levenston et al. 1997; Levenston et al. 1998; Levenston et al. 1999; Masaro and Zhu 1999).

In spite of the fact that numerous studies have been done on the solute transport in porous media and the theoretical framework for solute transport in porous materials is established (Bird et al. 2002; Brenner and Edwards 1993; Bird et al. 2002), many fundamental questions relating to solute transport in porous media have not been answered satisfactorily. For instance, what is the convective velocity of solute in tissue? How does this velocity relate to solvent velocity? What is the intrinsic diffusion coefficient (or diffusivity) of solute in charged porous media? How does mechanical loading affect solute transport in tissue? To address these questions, a mechano-electrochemical mixture theory(Lai et al. 1991; Gu et al. 1998) was used in this study. The objectives of this study were: (1) to develop a transport theory specific for charge hydrated soft tissues (e.g., cartilaginous tissue) using a mixture theory approach and (2) to analyze the effect of mechanical loading on the diffusion of solute in cartilage.

THEORY

The details of mechano-electrochemical mixture theory can be found in (Lai et al. 1991; Gu et al. 1998; Huyghe and Janssen 1997). Briefly, it models a charged hydrated soft tissue as a continuum mixture consisting of intrinsically incompressible solid phase, interstitial water phase, and solute phases. The driving forces for the transport of interstitial water and solutes are the gradients of (electro)chemical potentials. At any point within the mixture, an electro-neutrality is assumed. In the following analysis, only an isotropic case was considered.

Convective flux and diffusive flux of solute in porous media

Under a quasi-static condition, the momentum equation for each of the fluid phases (water and solutes) within a porous medium (mixture) is given as follows (Lai et al. 1991; Gu et al. 1998):

$$-\rho^{\alpha}\nabla\overset{\sim}{\mu}^{\alpha}+\sum_{\beta}f_{\alpha\beta}\left(\mathbf{v}^{\beta}-\mathbf{v}^{\alpha}\right)=0\ (\text{for}\ \alpha\neq\text{solid phase}), \tag{1}$$

where ρ^{α} is the apparent mass density, $\tilde{\mu}^{\alpha}$ is electrochemical potential (per unit mass), and $\mathbf{v}^{\alpha}$ is the velocity of fluid (solvent or solute) phase α, $f_{\alpha\beta}$ is the drag coefficient (per unit of mixture volume) between α and β phases with $f_{\alpha\beta}=f_{\beta\alpha}$ and $f_{\alpha\beta}\equiv 0$ if α=β. In equation (1), the summation is carried out for β over all phases (including solid phase). For solutes, the apparent mass density (ρ^{α}) is related to solute molar weight (M^{α}) and solute concentration (c^{α}, in moles per unit volume of solvent) by

$$\rho^{\alpha}=\phi^{w}M^{\alpha}c^{\alpha}, \tag{2}$$

where ϕ^{w} is the volume fraction of water (solvent). Solving for $\mathbf{v}^{\alpha}$ from equation (1), one obtains (Gu et al. 1998)

$$\mathbf{v}^{\alpha}=\left(\sum_{\beta} f_{\alpha\beta}\,\mathbf{v}^{\beta}-\rho^{\alpha}\nabla\tilde{\mu}^{\alpha}\right)/d_{\alpha}, \tag{3}$$

where

$$d_{\alpha}=\sum_{\beta} f_{\alpha\beta}. \tag{4}$$

Equation (3) can be written as

$$\mathbf{v}^{\alpha}=\mathbf{v}_{c}^{\alpha}-\rho^{\alpha}\nabla\tilde{\mu}^{\alpha}/d_{\alpha} \tag{5}$$

where

$$\mathbf{v}_{c}^{\alpha}\equiv\sum_{\beta} f_{\alpha\beta}\mathbf{v}^{\beta}/d_{\alpha}. \tag{6}$$

Equation (5) states that any solvent or solute velocity ($\mathbf{v}^{\alpha}$ is equal to the sum of its convective velocity ($\mathbf{v}_{c}^{\alpha}$) and its diffusive velocity resulted from the negative gradient of its (electro) chemical potential (second term on the right hand side of equation 5). The convective velocity ($\mathbf{v}_{c}^{\alpha}$), see equation (6), is equal to the weighted mean velocity of other constituents since $f_{\alpha\beta}\equiv 0$ for α=β (i.e., independent of $\mathbf{v}^{\alpha}$ itself). Note that the value of the convective velocity ($\mathbf{v}_{c}^{\alpha}$) depends on the choice of a reference frame (i.e., it is not objective). This means that one could choose a particular frame of reference such that the convective velocity for α-phase is zero.

The diffusive molar flux ($\mathbf{J}_{D}^{\alpha}$) for α-phase is defined as

$$\mathbf{J}_{D}^{\alpha}\equiv\phi^{w}c^{\alpha}\left(\mathbf{v}^{\alpha}-\mathbf{v}_{c}^{\alpha}\right) \tag{7}$$

Using equation (5), one obtains

$$\mathbf{J}_{D}^{\alpha}=-\phi^{w}c^{\alpha}\rho^{\alpha}\nabla\tilde{\mu}^{\alpha}/d_{\alpha} \tag{8}$$

The intrinsic diffusion coefficient of solute (or solute diffusivity, D^{α}) in mixture is defined as

$$\mathbf{J}_{D}^{\alpha}\equiv-D^{\alpha}\rho^{\alpha}\nabla\tilde{\mu}^{\alpha}/RT \tag{9}$$

where R is the universal gas constant; T is the absolute temperature. This definition for solute intrinsic diffusivity is consistent with that in the literature [e.g., (Deen 1998)]. It follows from equations (8) and (9) that,

$$D^{\alpha}=RT\phi^{w}c^{\alpha}/d_{\alpha} \tag{10}$$

Note that the intrinsic solute diffusivity defined by equation (9) or equation (10) is independent of solute activity (or partition) coefficient or electrical charge effects (these will be further discussed in a separate paper). For a binary system (with solute α and water only), the convective velocity ($\mathbf{v}_c^\alpha$) in equation (6) reduces to $\mathbf{v}_c^\alpha = \frac{f_{\alpha w}\mathbf{v}^w}{f_{\alpha w}} = \mathbf{v}^w$, and solute diffusivity (D_o^α in solution) reduces to (with ϕ^w=1)

$$D_o^\alpha = RTc^\alpha / (f_{\alpha w})_o, \tag{10a}$$

where $(f_{\alpha w})_o$ is the drag coefficient between solute and water in the solution. Equation (10a) is the well-known Stokes-Einstein equation.

The solvent and solute velocities as well as their corresponding convective velocities (see equation 6) depend on the frame of reference. For the purpose of investigating solute transport in porous media (mixture), it is necessary to use an objective quantity to describe the convective effect on solute transport. It seems natural to choose the relative solute flux (relative to the solid phase) to describe the solute transport in mixture. In this study, we use the relative molar solute flux ($\mathbf{J}^\alpha$), defined as

$$\mathbf{J}^\alpha \equiv \phi^w c^\alpha (\mathbf{v}^\alpha - \mathbf{v}^s), \tag{11}$$

where $\mathbf{v}^s$ is the velocity of solid phase. The relative flux defined in equation (11) is objective, independent of the frame of reference.

Using equations (5,7,9), the relative solute flux can be expressed as

$$\mathbf{J}^\alpha = \phi^w c^\alpha (\mathbf{v}_c^\alpha - \mathbf{v}^s) - D^\alpha \rho^\alpha \nabla \tilde{\mu}^\alpha / RT, \tag{12}$$

Introducing $\varepsilon^\alpha = \exp\left[M^\alpha \left(\tilde{\mu} - \mu_0^\alpha \right) / RT \right]$ for modified chemical potential of solute α (μ_0^α is the reference chemical potential) (Sun et al. 1999), equation (12) can be written as

$$\mathbf{J}^\alpha = \phi^w c^\alpha (\mathbf{v}_c^\alpha - \mathbf{v}^s) - \frac{\phi^w c^\alpha D^\alpha}{\varepsilon^\alpha} \nabla \varepsilon^\alpha \tag{13}$$

The first term on the right hand side of equations (12) and (13), defined as the relative convective flux J_{RC}^α, represents solute transport due to convection (relative to solid phase) and the second term (i.e., diffusive flux J_D^α) represents solute transport due to diffusion (and/or electrophoresis if the solute is charged).

The relative importance of convection to diffusion can be estimated by the Peclet number (Pe) defined as the ratio of convective flux to diffusive flux. Recall equation (13), one may define the Peclet number for solute α in mixture by

$$(Pe)^\alpha = \frac{\left| \mathbf{v}_c^\alpha - \mathbf{v}^s \right| L}{D^\alpha}, \tag{14}$$

where L is the characteristic length over which solute diffuses. Using equations (4,6,10), equation (14) can also be expressed in terms of drag coefficients and relative velocities:

$$(Pe)^{\alpha}=\frac{\left|\sum_{\beta} f_{\alpha\beta}\left(\mathbf{v}^{\beta}-\mathbf{v}^{s}\right)\right| L}{RT\phi^{w}c^{\alpha}}. \tag{15}$$

From equation (15), one can see that the Pe number defined by equation (14) does not explicitly depend on the drag coefficient between solute α and solid phase ($f_{\alpha s}$).

Consider a case where a cartilaginous tissue (mixture) consists of solid matrix (s), water (w), Na^{+} (+), Cl^{-} (−), and neutral soluble molecule (o) only. If the frictional interactions among solutes are assumed to be negligible, equation (6) reduces to

$$\mathbf{v}_{c}^{\alpha}=\frac{f_{\alpha w}\mathbf{v}^{w}+f_{\alpha s}\mathbf{v}^{s}}{f_{\alpha w}+f_{\alpha s}}\ (\text{for } \alpha=+,-,\text{o}). \tag{16}$$

So the relative velocity ($\mathbf{v}_{c}^{\alpha}-\mathbf{v}^{s}$) in equation (12) or equation (13) becomes

$$\mathbf{v}_{c}^{\alpha}-\mathbf{v}^{s}=\frac{f_{\alpha w}\,\mathbf{v}^{w}+f_{\alpha s}\,\mathbf{v}^{s}}{f_{\alpha w}+f_{\alpha s}}-\mathbf{v}^{s}=\frac{f_{\alpha w}}{f_{\alpha w}+f_{\alpha s}}\left(\mathbf{v}^{w}-\mathbf{v}^{s}\right)=H^{\alpha}\left(\mathbf{v}^{w}-\mathbf{v}^{s}\right), \tag{17}$$

where

$$H^{\alpha}=\frac{f_{\alpha w}}{f_{\alpha w}+f_{\alpha s}}\quad(\text{for } \alpha=+,-,\text{o}). \tag{18}$$

Introducing $\mathbf{J}^{w}[\equiv\phi^{w}(\mathbf{v}^{w}-\mathbf{v}^{s})]$ for water flux relative to solid matrix, equation (13) together with equation (17) can be written as

$$\mathbf{J}^{\alpha}=H^{\alpha}c^{\alpha}\mathbf{J}^{\mathbf{w}}-\frac{\phi^{w}c^{\alpha}D^{\alpha}}{\varepsilon^{\alpha}}\nabla\varepsilon^{\alpha}\quad(\text{for } \alpha=+,-,\text{o}), \tag{19}$$

The parameter H^{α} in equations (17,18,19) is equal to the ratio of relative convective speed to relative solvent speed (see equation 17). Thus, this parameter may be called the *convective coefficient* or convection coefficient (Evans and Quinn 2005). This coefficient is also known as the *hindrance factor* in the literature. It represents the hindrance effect on convection due to hydrodynamic and steric interactions between solute and solid matrix (Deen 1987; Johnston and Deen 1999). Obviously, from equation (18), the value of the convective coefficient (H^{α}) is equal to unity for a binary solution system (without solid phase). In porous media, the value of H^{α} is offen less than unity. It approaches unity when $f_{\alpha s} << f_{\alpha w}$.

Under the same assumption that the frictional interactions among solutes are negligible, the solute diffusivity in tissue is

$$D^{\alpha}=\frac{RT\phi^{w}c^{\alpha}}{f_{\alpha w}+f_{\alpha s}}\quad(\text{for } \alpha=+,-,\text{o}). \tag{20}$$

The corresponding Pe number for solute α is:

$$(Pe)^{\alpha}=\frac{H^{\alpha}\,|\mathbf{J}^{w}|\,L}{\phi^{w}D^{\alpha}}=\frac{f_{\alpha w}\,|\mathbf{v}^{w}-\mathbf{v}^{s}|\,L}{RT\phi^{w}c^{\alpha}}\quad(\text{for }\alpha=+,-,o)\,. \tag{21}$$

Drag coefficients in tissue ($f_{\alpha w}$ and $f_{\alpha s}$)

Little information on the value of H^{α} (for α=+,−,o) is available in literature for cartilaginous tissues(Evans and Quinn 2005). The drag coefficients ($f_{\alpha w}$) between solute (α) and water (w) in tissue (mixture) are in general not equal to that in solution. Based on equation (19), one can design an experiment for determining the value of H^{α}(Evans and Quinn 2005). After measuring H^{α} and D^{α}, one can determine the drag coefficients $f_{\alpha w}$ and $f_{\alpha s}$ in the tissue using equations (18 and 20). For example, the drag coefficient between solute and water per unit volume of interstitial water ($f_{\alpha w}/\phi^{w}$) in the tissue can be calculated by equations (18) and (20) as follows:

$$\frac{f_{\alpha w}}{\phi^{w}}=\frac{RTc^{\alpha}H^{\alpha}}{D^{\alpha}}. \tag{22}$$

Using equation (10a), the ratio of drag coefficient between solute (α) and water (per volume of interstitial water) in tissue to that in solution at the same solute concentration is given by

$$\frac{f_{\alpha w}}{\phi^{w}(f_{\alpha w})_{o}}=\frac{H^{\alpha}}{D^{\alpha}/D_{o}^{\alpha}}. \tag{23}$$

For most cases, it is reasonable to speculate that $\frac{f_{\alpha w}}{\phi^{w}(f_{\alpha w})_{o}}\geq 1$, therefore,

$$\frac{D^{\alpha}}{D_{o}^{\alpha}}\leq H^{\alpha}\leq 1. \tag{24}$$

The equal sign in the above equation may be used for limiting cases. Note that the above inequality does not hold for those solutes that could diffuse faster in porous media than in water.

Knowledge of these coefficients can provide an insight into the mechanisms of solute transport in tissue at molecular (nano) level.

Strain-dependent solute diffusivity

In this study, the following constitutive relationship was used for the intrinsic solute diffusivity (Gu et al. 2004):

$$\frac{D^{\alpha}}{D_{0}^{a}}=\exp\left[-a_{1}\left(\frac{r_{s}^{a}}{\sqrt{\kappa}}\right)^{b_{1}}\right],\quad(\text{for }\alpha=+,-,o) \tag{25}$$

where a_1 and b_1 are two positive parameters that depend on the structure of tissue, r_s^a is the Stokes radius of the solute α, and κ is the Darcy permeability which is related to the hydraulic permeability (k) by κ=kη (η is the fluid viscosity). The Darcy permeability is porosity-dependent, given as follows(Gu et al. 2003),

$$\kappa = a_2 \left(\frac{\phi^w}{\phi^s} \right)^{b_2}, \tag{26}$$

where a_2 and b_2 are two positive parameters which again depend on the structure of tissue. Since tissue porosity (ϕ^w) is related to tissue dilatation (e) and the porosity ϕ_o^w at the reference configuration (i.e., at e=0) by: (Lai et al. 1991)

$$\phi^w = \frac{\phi_o^w + e}{1+e}, \tag{27}$$

both intrinsic hydraulic permeability and intrinsic solute diffusivity are strain-dependent.

ANALYSIS OF SOLUTE DESORPTION IN CARTILAGE UNDER DYNAMIC COMPRESSION

Desorption of uncharged solute from cartilage explants under unconfined compression was simulated in this study (Fig. 1). In the simulation, a cylindrical cartilage sample with 1mm thickness (h) and 1.5mm radius (R) is placed between two rigid, flat, frictionless and impermeable loading platens. The tissue is initially equilibrated with a bathing solution of 0.15M NaCl containing 0.04mM uncharged solute (its size is similar to IGF-1), followed by a ramp compression (10% or 20% offset strain in 100s). After reaching equilibrium at this new configuration (relaxation time=50,000s), the bathing solution is changed to the normal saline (without uncharged solute), and a dynamic compression (2.5% or 5% dynamic amplitude at 0.001, 0.01 or 0.1 Hz) is simultaneously applied to the tissue. Solute desorption from cartilage sample takes place only in the radial direction.

The cartilage tissue was modeled as an isotropic homogeneous mixture of intrinsically incompressible elastic solid phase, water phase, ion (Na^+ and Cl^-) and uncharged solute phase. The governing equations for the mixture are summarized in Appendix. Note that strain-dependent diffusivity (i.e., equation 25) and permeability (i.e., equation 26) were considered in this simulation. Due to the symmetry with respect to r=0 and z=0, only upper quadrant of the sample was modeled for this 2D problem of interest.

Initial condition

$$t=0: \quad u=0, \quad \varepsilon^w=\varepsilon^{w^*}, \quad \varepsilon^+=\varepsilon^{+^*}, \quad \varepsilon^-=\varepsilon^{-^*}, \quad \varepsilon^o=\varepsilon^{o^*}, \tag{28}$$

where superscript * stands for the quantities in the bathing solution. In this study, the free-swelling (i.e., unloaded) state of tissue equilibrated with the bathing solution was chosen as the reference configuration for strain.

Boundary condition

$$r=0: \quad u_r=\sigma_{rz}=0, \quad J_r^w=J_r^+=J_r^-=J_r^o=0; \tag{29}$$

$$r=\mathrm{R}:\sigma_{rr}=\sigma_{rz}=0,\ \varepsilon^{w}=\varepsilon^{w^*},\varepsilon^{+}=\varepsilon^{+^*},\varepsilon^{-}=\varepsilon^{-^*},\varepsilon^{o}=\varepsilon^{o^*}-\varepsilon^{o^*}H(t-t_1); \tag{30}$$

$$\mathrm{z}=0:\quad u_z=\sigma_{rz}=0,J_z^w=J_z^+=J_z^-=J_z^o=0; \tag{31}$$

$$\mathrm{z}=\mathrm{h}/2:\quad u_z=-u(t),\ \sigma_{rz}=0,\ J_z^w=J_z^+=J_z^-=J_z^o=0; \tag{32}$$

where (see Figure 1)

$$\begin{aligned} u(t) &= u_o t/t_o \quad \text{for } \mathrm{t}<\mathrm{t}_o,\\ u(t) &= u_o \quad \text{for } \mathrm{t}_o\le \mathrm{t}<\mathrm{t}_1,\text{or}\\ u(t) &= u_o+u_1\sin\left[2\pi f(t-t_1)\right]\cdot H(t-t_1) \quad \text{for } \mathrm{t}\ge \mathrm{t}_1. \end{aligned} \tag{33}$$

Here H(t) is the Heaviside step function satisfying H(t)=0 for t<0 and H=1 for t≥ 0.

Numerical Method

A mixed finite element formulation of Sun et al (1999) was adopted to solve this 2D axial symmetric initial- and boundary-value problem using FEMLAB software (FEMLAB3.1, COSMOL Inc., Burlington, MA). The details of the numerical implementation can be found in our previous publication (Yao and Gu 2004). A mesh of 813 second-order triangle Lagrange elements was used in this analysis. The maximum time-step of 1s was used during the ramp phase, and variable maximum time-steps from 0.05s to 10s were used during the relaxation phase. During sinusoidal compression, at least 32 time steps had been taken for each cycle. The convergence of the numerical model was examined by refining the mesh and tightening the tolerance. The numerical accuracy was checked against the 2D triphasic stress-relaxation problem published in the literature (Sun et al. 2004; Sun 2002).

The following baseline parameters were used in the simulation: temperature T=298K, bathing solution c*=0.15 M NaCl, initial water content $\phi^w{}_0$=0.8, Lame coefficients λ=0.1MPa and μ=0.2MPa, coupling coefficient B_w=0, initial fixed charge density $c^F{}_0$=0.2mEq/ml(Mow et al. 2002). The values of a_1=1.25 and b_1=0.681 were used in the constitutive equation of solute diffusivity, i.e., equation (25) (Gu et al. 2004). The Stokes radii of cation (Na^+) $r_s{}^+$=0.197nm, anion (Cl^-) $r_s{}^-$=0.142, and uncharged solute radius $r_s{}^o$=1.146nm were calculated based on the corresponding diffusivity value in the aqueous solution at 25°C using Stokes-Einstein equation. For uncharged solute, the diffusivity is similar to the values of IGF-1 and the partition coefficient is Φ=0.1. For small ions, activity coefficient $\gamma_\pm/\gamma^*_\pm$=1 and osmotic coefficient ϕ=1 were used. In this study, the values of these parameters were assumed to be unity except for the cases where the effect of convective coefficient on solute transport is investigated (see Figure 6). To calculate Darcy permeability, the values of a_2=0.00339nm^2 and b_2=3.24 were used in equation (26) (Gu et al. 2003). Note that initial neutral solute concentration $c^o{}_i=4\times10^{-5}$ mol/m^3, permeability $k_0=5\times10^{-16}$m^4/Ns, and aggregate modulus H_A=0.5MPa were used for variable normalization. All results are presented at z=0, since they are independent of the depth under frictionless boundary condition (Armstrong et al. 1984).

NUMERICAL RESULTS

1. Effect of static compression on solute diffusion

With static compression only, an increase in static compression strain reduced solute diffusion within the cartilage sample, as shown in the concentration distributions within the tissue (Fig. 2). This retarded diffusion is mainly due to the decrease in solute diffusivity governed by equation (25), in which reducing tissue permeability will decrease solute diffusivity. Static compression decreased the permeability by reducing tissue water content (equation 26).

2. Effect of dynamic loading phase on solute concentration distribution

The normalized solute concentration distribution in tissue sample apparently depended on the loading phase of dynamic compression. The concentration distributions near the radial edge of the explant exhibited a concave shape at the peak phase as well as a convex shape at the valley phase (Fig. 3). This phenomenon is mainly due to the oscillatory dilatation change in the radial edge of the explant during dynamic compression (Fig. 4).

3. Effect of dynamic compression strain on solute desorption

Increasing dynamic compression strain from 2.5% to 5% has little effect on the concentration distribution at neutral phase (Fig. 5) under unconfined compression with frictionless boundary.

4. Effect of convective coefficient on solute concentration distribution

The contribution of fluid convection to total solute transport is regulated by the convective coefficient according to equation (19). Figure 6 shows that convective coefficient has no effect on solute concentration distribution for this case.

This is mainly because the relative convective flux J^o_{RC} (Fig. 7) is much smaller than diffusive flux J^o_D (Fig. 8), even though the magnitude of absolute convective flux J^o_{AC} $\left(=J^o_{RC}+\phi^w c^o \mathbf{v}^{\mathbf{s}}\right)$ is very high (Fig. 9).

5 Effect of loading frequency on diffusive flux and relative convective flux

The effect of loading frequency on solute desorption was also investigated (Fig 10). While having little effect on the magnitude of relative convective flux (Fig. 11), an increase in loading frequency slightly increased diffusive flux (Fig. 12), resulting in a lower concentration profile near the radial edge of the explant (Fig.10). Note that the magnitude of the diffusive flux depends on the loading phase as well (not shown).

DISCUSSION

Using the mechano-electrochemical mixture theory, the transport theory for charged hydrated soft tissues was developed (Objective #1). The theoretical analyses clearly show that in porous media, the convective velocity is in general not equal to the solvent velocity. It is the convective velocity relative to the solid phase (i.e., the relative convective velocity) that governs the convection of solute transport in the porous media. This notion is further confirmed by our numerical analyses on solute desorption in cartilage under unconfined dynamic compression (Objective #2).

Unlike the traditional treatment on convection and diffusion in porous media [e.g., (Truskey et al. 2004)], in the present study, the convective velocity for solute α is defined as the mean velocity of other phases (or species) weighed by the drag coefficients between solute α and other constituents. This definition means that the convective velocity for each solute phase is different. The diffusive velocity for phase α is defined as the difference between its velocity

to its convective velocity. This naturally leads to a uniform, mathematic expression for the diffusive flux [equations (9)] for all solute phases in mixture. That is, the diffusive flux for each solute phase in the mixture is resulted from the sole gradient of its (electro)chemical potential. The corresponding diffusivity [equations (9) and (10)] is intrinsic, and independent of electrical charge effect even though the solute is charged. This result [equation (10)] is consistent with the well-known Stokes-Einstein equation for diffusivity. This concept of intrinsic diffusivity has been successfully used in our recent experiments on the determination of ion diffusivity in agarose gels (Gu et al. 2004).

In our numerical analyses, dynamic loading has little effect on solute desorption. This is mainly due to the relatively low dynamic strain. When the dynamic strain is increased to 20%, the effect of dynamic loading on the transport of large solute is more pronounced (Figure 13). At low strain levels ($\leq 5\%$), the relative convective flux is much smaller than the diffusive flux (see Figs. 7 and 8), indicating the Pe number is much smaller than unity. Note that at high strain levels, the dynamic loading always enhances solute transport. For instance, one could compress the tissue to zero-water content then release it. It is obvious that the enhanced transport in such a dynamic compression test depends on loading frequency. This analysis is consistent with experimental and theoretical reports in literature (Mauck et al. 2003; O'Hara et al. 1990; Quinn et al. 2002).

Quinn et al (2002) reported that during unconfined dynamic compression of a cartilage sample (disk), the distribution of solute concentration in the radial direction is concave near the radial edge of the cartilage sample. Our simulation (Fig. 13) is consistent with this finding. Note that in our simulations, the convective coefficient for large solute (i.e., IGF-1) is assumed to be unity. This assumption has little effect on solute transport when convection is negligible (i.e., $Pe<<1$). However, when convection effect is not negligible (e.g., $Pe>1$), more exact characterizations of strain-dependent convective coefficient as well as strain-dependent solute diffusivity are important for investigating solute transport in dynamically compressed tissues (Evans and Quinn 2005).

CONCLUSIONS

In this study, a theory for solute transport in porous media is developed using the mechano-electrochemical mixture theory. The convective and diffusive fluxes of solute in such a material have been clearly defined [Equations (6) and (7)]. The relationship between convective velocity and drag coefficients has been presented. Analyses show that the convective velocity for each of solute phases is different [Equation (6)]. It is the convective velocity relative to solid phase that governs the convection of solute transport in porous media. The diffusive flux is proportional to the negative gradient of its (electro)chemical potential. The proportional parameter between the diffusive flux and the gradient of (electro)chemical potential is related to the intrinsic solute diffusivity [Equation (9)]. This theory has been applied to analyze numerically the effect of dynamic mechanical compression on solute desorption in cartilage. Numerical simulations show that at low strain levels ($\leq 5\%$), dynamic loading has little effect on large solute (i.e., IGF-1) transport in cartilage explant in the unconfined compression experiment. This study provides an important insight into solute transport in charged hydrated soft tissues and biomaterials.

Acknowledgement

This work was support by the grants from the NIH (AR46860 and AR050609).

Appendix

The balance of linear momentum for the mixture and the conservation of mass for each of phases or species led to the following governing equations (Gu et al. 1998; Lai et al. 1991; Sun et al. 1999; Yao 2004):

$$\nabla \cdot \sigma = 0, \tag{A1}$$

$$\nabla \cdot (\mathbf{v}^{\mathrm{s}} + \mathbf{J}^{\mathrm{w}}) = 0, \tag{A2}$$

$$\partial (\phi^w c^\alpha) / \partial t + \nabla \cdot (\mathbf{J}^\alpha + \phi^w c^\alpha \mathbf{v}^{\mathrm{s}}) = 0, \alpha = +, -, o \tag{A3}$$

$$\mathbf{v}^{\mathrm{s}} = \frac{\partial \mathbf{u}}{\partial t}, \tag{A4}$$

$$\sigma = -\left[RT\varepsilon^w + RT\phi (c^+ + c^- + c^o) - p_o\right] + (\lambda + B_w) \nabla \cdot \mathbf{u} + \mu \left[\nabla \mathbf{u} + (\nabla \mathbf{u})^T\right], \tag{A5}$$

$$\mathbf{J}^{\mathrm{w}} = -RTk\left(\nabla \varepsilon^w + \frac{c^+}{\varepsilon^+} H^+ \nabla \varepsilon^+ + \frac{c^-}{\varepsilon^-} H^- \nabla \varepsilon^- + \frac{c^o}{\varepsilon^o} H^o \nabla \varepsilon^o\right), \tag{A6}$$

$$\mathbf{J}^\alpha = H^\alpha c^\alpha \mathbf{J}^{\mathrm{w}} - \frac{\phi^w c^\alpha D^\alpha}{\varepsilon^\alpha} \nabla \varepsilon^\alpha, (\alpha = +, -, o) \tag{A7}$$

where σ is the total stress tensor of the mixture, **u** is the solid displacement, ε^{w} is modified water chemical potential, ϕ is the osmotic coefficient; p_o is the pre-stress [see equation (A8) below]; B_w is the interphase coupling coefficient; λ and μ are Lame coefficients of solid matrix; k is the intrinsic (i.e. closed-circuit) permeability; D^+, D^- and D^o are the intra-tissue diffusivities of cation, anion and uncharged solute, respectively.

In arriving at equations (6 and 7), infinitesimal deformation assumption was made (Lai et al. 1991;Sun et al. 1999). Note that the mechanical interactions among solutes were assumed to be negligible(Yao 2004). More general cases can be found in (Gu et al. 1998;Yao 2004) The value of pre-stress (p_o) in equation (A5) depends on the choice of the reference configuration for strain. In this study, the free-swelling state of tissue equilibrated with the bathing (NaCl) solution of concentration c^* (no other uncharged solute) was chosen as the reference configuration for strain. Thus, the pre-stress (p_o) was given as

$$p_o = RT\left[\phi (c_o^+ + c_o^-) - 2\phi^* c^*\right] - B_w e_o, \tag{A8}$$

where c_o^+ and c_o^- are the ion concentrations within the tissue at equilibrium (i.e., the initial ion concentrations), and e_o is the dilatation of tissue at equilibrium (relative to the hypertonic state). If one chooses the tissue configuration at the hypertonic state (load-free) as the reference configuration, then p_o=0 and e_o=0. In our calculations, all strains were relative to the free-swelling state of tissue equilibrated with 0.15M NaCl bathing solution (Gu et al. 1993).

In equations (A6, A7), the modified (electro)chemical potentials (ε^w, ε^+, ε^-, ε^o) were related to fluid pressure (p), electrical potential (ψ), and solute concentrations (c^+, c^-, c^o) by (Sun et al. 1999):

$$\varepsilon^w=\frac{p}{RT}-\phi\left(c^++c^-+c^o\right)+\frac{B_w}{RT}e, \tag{A9}$$

$$\varepsilon^\alpha=\gamma_\alpha c^\alpha \exp\left(\frac{z_\alpha F_c\psi}{RT}\right),\mathrm{a}=+,-,\mathrm{o} \tag{A10}$$

where e is the dilatation; F_c is the Faraday constant; γ_α and z_α are the activity coefficients and valence, respectively. Note that the valence for neutral solute is zero. At equilibrium, the activity coefficient of the uncharged solute within the tissue (γ_o) was related to the partition coefficient (Φ) (i.e., the ratio of solute concentration in tissue to solute concentration in bathing solute at equilibrium) and the activity coefficient of the uncharged solute in bathing solution (γ_o^*) by

$$\gamma_o=\gamma_o^*/\Phi. \tag{A11}$$

The ion concentrations were related to the value of negatively fixed charged density (c^F) through the electroneutrality condition in this model (Lai et al. 1991):

$$c^+=c^-+c^F, \tag{A12}$$

where c^F is related to the tissue porosity, the reference FCD (c_0^F) and reference porosity (ϕ_0^w) by

$$c^F=\frac{c_0^F\left(1-\phi^w\right)\phi_0^w}{\left(1-\phi_0^w\right)\phi^w}. \tag{A13}$$

References

Armstrong CG, Lai WM, Mow VC. An analysis of the unconfined compression of articular cartilage. J Biomech Eng 1984;106:165–173. [PubMed: 6738022]

Bird, RB.; Stewart, WE.; Lightfoot, EN. Transport Phenomena. John Wiley & Sons, Inc.; New York: 2002.

Bonassar LJ, Grodzinsky AJ, Srinivasan A, Davila SG, Trippel SB. Mechanical and physicochemical regulation of the action of insulin-like growth factor-I on articular cartilage. Arch.Biochem.Biophys 2000;379:57–63. [PubMed: 10864441]

Brenner, H.; Edwards, DA. Macrotransport processes. Butterworth-Heinemann; Stoneham, MA: 1993.

Burstein D, Gray ML, Hartman AL, Gipe R, Foy BD. Diffusion of small solutes in cartilage as measured by nuclear magnetic resonance (NMR) spectroscopy and imaging. J Orthop Res 1993;11:465–478. [PubMed: 8340820]

Deen, WM. Analysis of Transport Phenomena. Oxford University Press; New York: 1998.

Deen WM. Hindered transport of large molecules in liquid-filled pores. AIChE Journal 1987;33:1409–1425.

Evans RC, Quinn TM. Solute convection in dynamically compressed cartilage. Journal of Biomechanics. 2005in press

Ferguson SJ, Ito K, Nolte LP. Fluid flow and convective transport of solutes within the intervertebral disc. J Biomech 2004;37:213–221. [PubMed: 14706324]

Garcia AM, Frank EH, Grimshaw PE, Grodzinsky AJ. Contributions of fluid convection and electrical migration to transport in cartilage: relevance to loading. Arch.Biochem.Biophys 1996;333:317–325. [PubMed: 8809069]

Grodzinsky AJ. Electromechanical and physicochemical properties of connective tissue. Crit Rev.Biomed.Eng 1983;9:133–199. [PubMed: 6342940]

Gu WY, Lai WM, Mow VC. Transport of fluid and ions through a porous-permeable charged-hydrated tissue, and streaming potential data on normal bovine articular cartilage. J Biomech 1993;26:709–723. [PubMed: 8514815]

Gu WY, Lai WM, Mow VC. A mixture theory for charged-hydrated soft tissues containing multi-electrolytes: passive transport and swelling behaviors. Journal of Biomechanical Engineering 1998;120:169–180. [PubMed: 10412377]

Gu WY, Yao H, Huang C-Y, Cheung HS. New insight into deformation-dependent hydraulic permeability of gels and cartilage, and dynamic behavior of agarose gels in confined compression. J Biomech 2003;36:593–598. [PubMed: 12600349]

Gu WY, Yao H, Vega AL, Flagler D. Diffusivity of ions in agarose gels and intervertebral disc: Effect of porosity. Annals of Biomedical Engineering 2004;32:1710–1717. [PubMed: 15675682]

Horner HA, Urban JP. 2001 Volvo Award Winner in Basic Science Studies: Effect of nutrient supply on the viability of cells from the nucleus pulposus of the intervertebral disc. Spine 2001;26:2543–2549. [PubMed: 11725234]

Huyghe JM, Janssen JD. Quadriphasic mechanics of swelling incompressible porous media. Int J Engng Sci 1997;35:793–802.

Johnston ST, Deen WM. Hindered convection of proeins in agarose gels. Journal of Membrane Science 1999;153:271–279.

Lai WM, Hou JS, Mow VC. A triphasic theory for the swelling and deformation behaviors of articular cartilage. J Biomech Eng 1991;113:245–258. [PubMed: 1921350]

Leddy HA, Guilak F. Site-specific molecular diffusion in articular cartilage measured using fluorescence recovery after photobleaching. Annals of Biomedical Engineering 2003;31:753–760. [PubMed: 12971608]

Levenston ME, Eisenberg SR, Grodzinsky AJ. A variational formulation for coupled physicochemical flows during finite deformations of charged porous media. International Journal of Solids and Structures 1998;35:4999–5019.

Levenston ME, Frank EH, Grodzinsky A. Finite deformation theory and finite element formation for coupled electrokinetic and fluid flow in soft tissues: application to electroosmotic flow. ASME Adv in Bioeng 1997:187–188.

Levenston ME, Frank EH, Grodzinsky AJ. Electrokinetic and poroelastic coupling during finite deformations of charged porous media. Journal of Applied Mechanics 1999;66:323–333.

Maroudas, A. Physicochemical properties of articular cartilage. In: Freeman, MAR., editor. Adult Articular Cartilage. Pitman Medical; 1979.

Maroudas A. Biophysical chemistry of cartilaginous tissues with special reference to solute and fluid transport. Biorheology 1975;12:233–248. [PubMed: 1106795]

Masaro L, Zhu XX. Physical models of diffusion for polymer solutions, gels and solids. Progress in Polymer Science 1999;24:731–775.

Mauck RL, Hung CT, Ateshian GA. Modeling of neutral solute transport in a dynamically loaded porous permeable gel: Implications for articular cartilage biosynthesis and tissue engineering. Journal of Biomechanical Engineering 2003;125:602–614. [PubMed: 14618919]

Mow VC, Ratcliffe A, Poole AR. Cartilage and diarthrodial joints as paradiams for hierarchical materials and structures. Biomaterials 1992;13:67–97. [PubMed: 1550898]

Mow, VC.; Sun, DN.; Guo, XE.; Likhitpanichkul, M.; Lai, WM. Fixed negative charges modulate mechanical behavior and electrical signals in articular cartilage under unconfined compression - a triphasic paradigm. In: Ehlers, W.; Bluhm, J., editors. Porous media: theory, experiments and numerical application. Springer; Berlin: 2002.

Nimer E, Schneiderman R, Maroudas A. Diffusion and partition of solutes in cartilage under static load. Biophycal Chemistry 2003;106:125–146.

O'Hara BP, Urban JP, Maroudas A. Influence of cyclic loading on the nutrition of articular cartilage. Ann Rheum Dis 1990;49:536–539. [PubMed: 2383080]

Quinn TM, Kocian P, Meister JJ. Static compression is associated with decreased diffusivity of dextrans in cartilage explants. Arch Biochem Biophys 2000;384:327–334. [PubMed: 11368320]

Quinn TM, Morel V, Meister JJ. Static compression of articular cartilage can reduce solute diffusivity and partitioning: implications for the chondrocyte biological response. J Biomech 2001;34:1463–1469. [PubMed: 11672721]

Quinn TM, Studer C, Grodzinsky AJ, Meister JJ. Preservation and analysis of nonequilibrium solute concentration distributions within mechanically compressed cartilage explants. J Biochem Biophys Methods 2002;31:83–95. [PubMed: 12204413]

Sun, DN. Theoretical and experimental investigations of the mechano-electrochemical properties of articular cartilage, a charged-hydrated-soft, biological tissue. Columbia University; New York, NY: 2002. Ph.D. Dissertation

Sun DN, Gu WY, Guo XE, Lai WM, Mow VC. A mixed finite element formulation of triphasic mechano-electrochemical theory for charged, hydrated biological soft tissues. International Journal for Numerical Methods in Engineering 1999;45:1375–1402.

Sun DN, Guo XE, Likhitpanichkul M, Lai WM, Mow VC. The Influence of the fixed negative charges on mechanical and electrical behaviors of articular cartilage under unconfined compression. J Biomech Engng 2004;126:6–16. [PubMed: 15171124]

Torzilli PA, Adams TC, Mis RJ. Transient solute diffusion in articular cartilage. J Biomech 1987;20:203–214. [PubMed: 2437125]

Truskey, GA.; Fan, Y.; Katz, DF. Transport phenomena in biological systems. Pearson Education, Inc.; Upper Saddle River, NJ: 2004.

Urban JP, Holm S, Maroudas A. Diffusion of small solutes into the intervertebral disc: as in vivo study. Biorheology 1978;15:203–221. [PubMed: 737323]

Yao, H. Physical signals and solute transport in cartilaginous tissues. University of Miami; Coral Gables, FL: 2004. Ph.D. Dissertation

Yao H, Gu WY. Physical signals and solute transport in cartilage under dynamic unconfined compression: finite element analysis. Annals of Biomed Engng 2004;32:380–390.

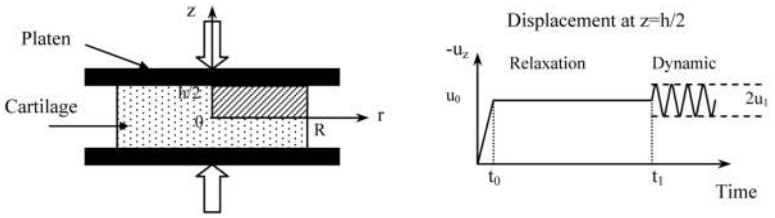

Figure 1.
Schematic of dynamic unconfined compression test configuration for solute desorption experiment. A ramp compression (10% or 20% offset strain) was applied in 100s. After stress relaxation in 50000s, a dynamic compression (2.5% or 5% dynamic strain) was imposed.

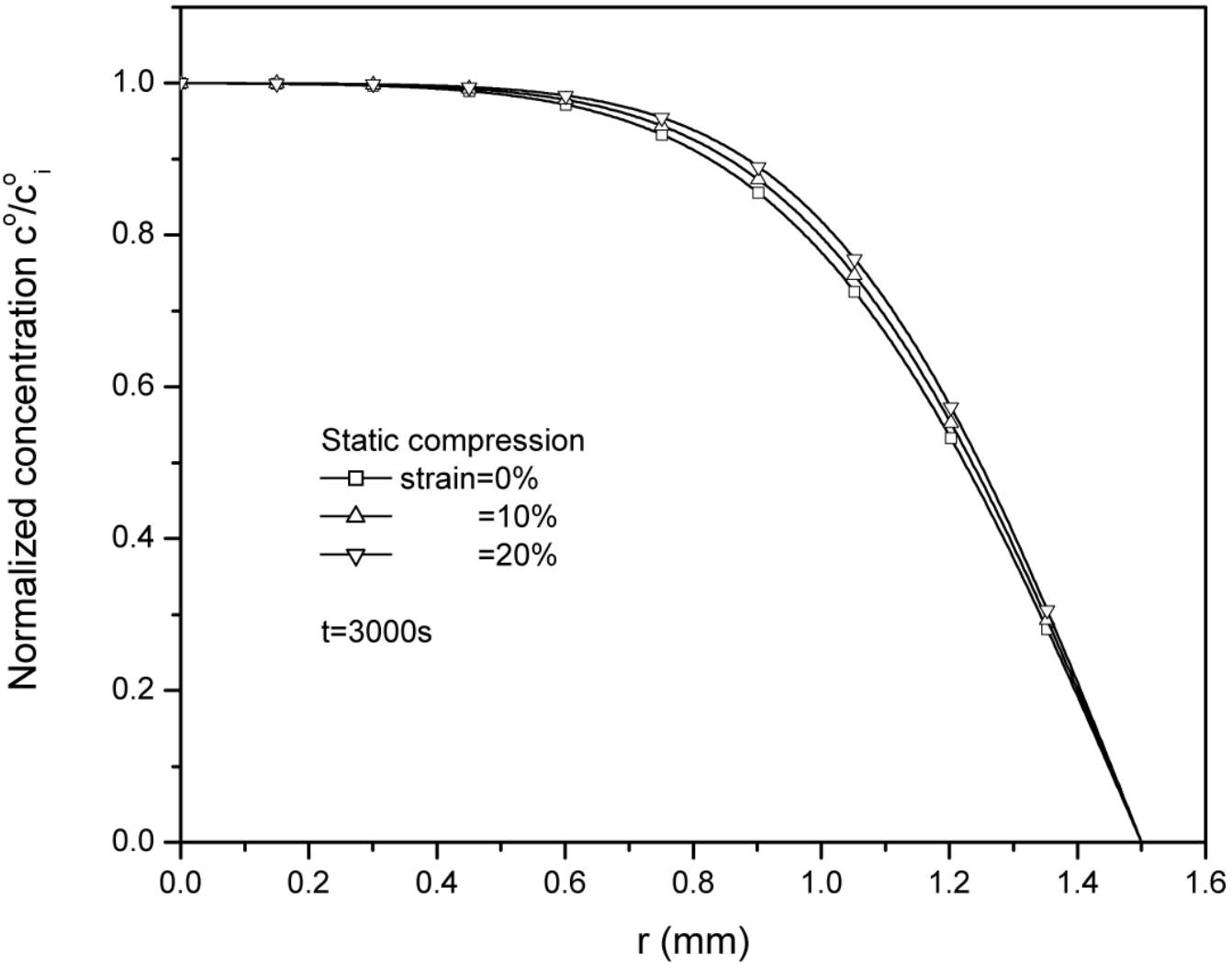

Figure 2.
Solute concentration c^o (normalized by solute concentration in tissue at t=0, c^o_i) distributions within the tissue after 3000s of radial desorption under 0%, 10% and 20% static compression.

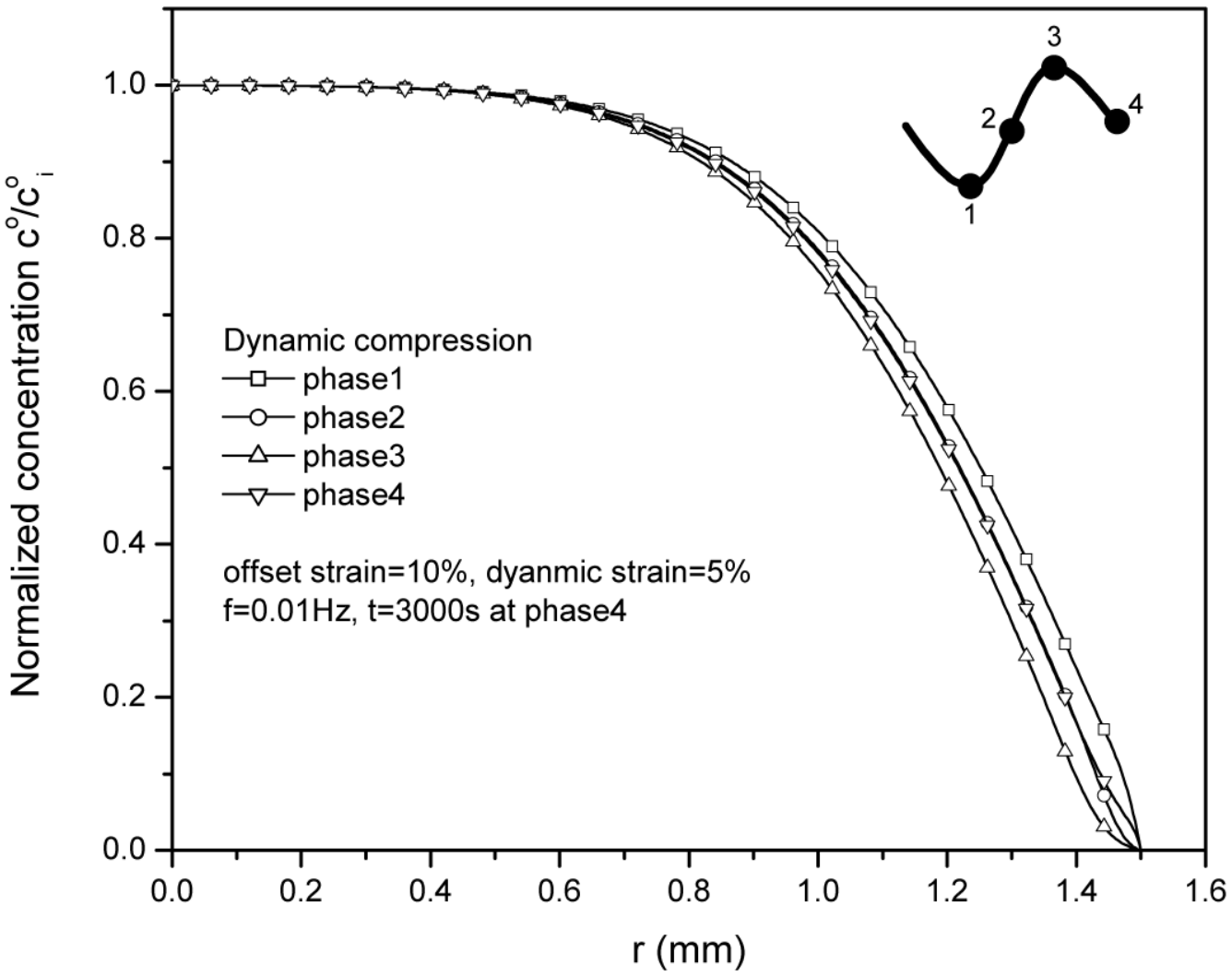

Figure 3.
Solute concentration distributions within the tissue during 30th cycle at 5% dynamic compression of 0.01Hz. The concentration distributions depend on the loading phase.

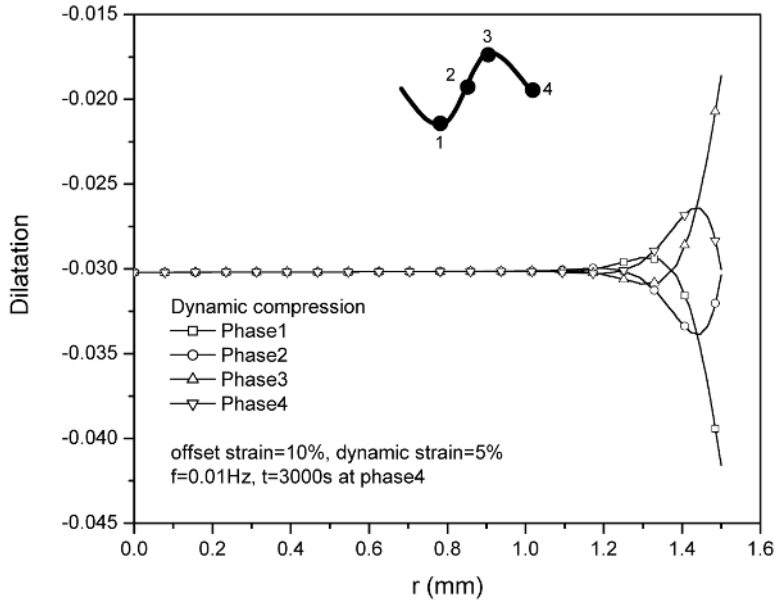

Figure 4.
Tissue dilatation profiles during 30th cycle at 5% dynamic compression of 0.01Hz.

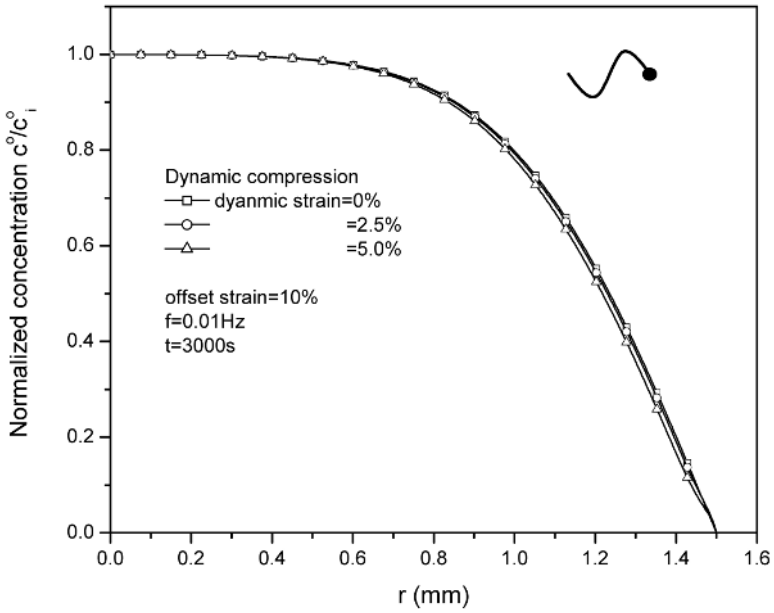

Figure 5.
Effect of dynamic compression (0%, 2.5% and 5%) on solute concentration distributions within the tissue at t=3000s. The loading frequency is 0.01Hz.

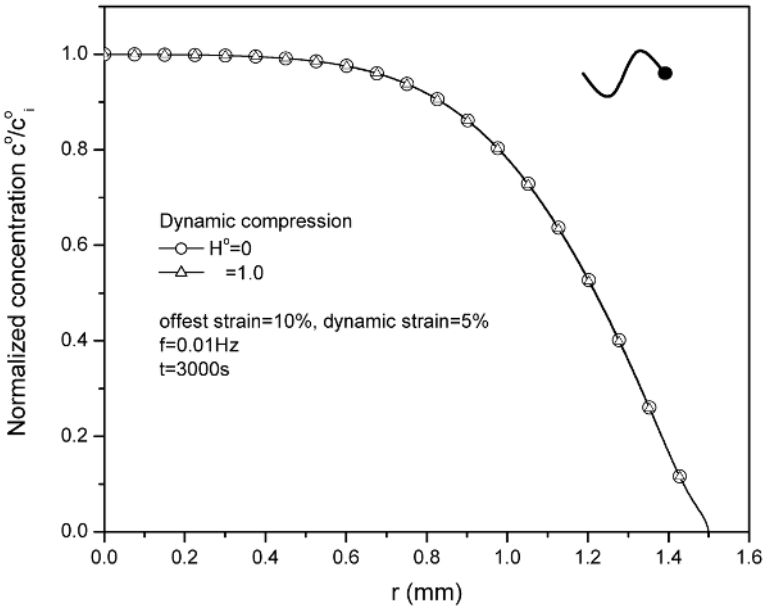

Figure 6.
Effect of convective coefficient (H^o) on solute concentration distributions (t=3000s) within the tissue at 5% dynamic strain of 0.01Hz.

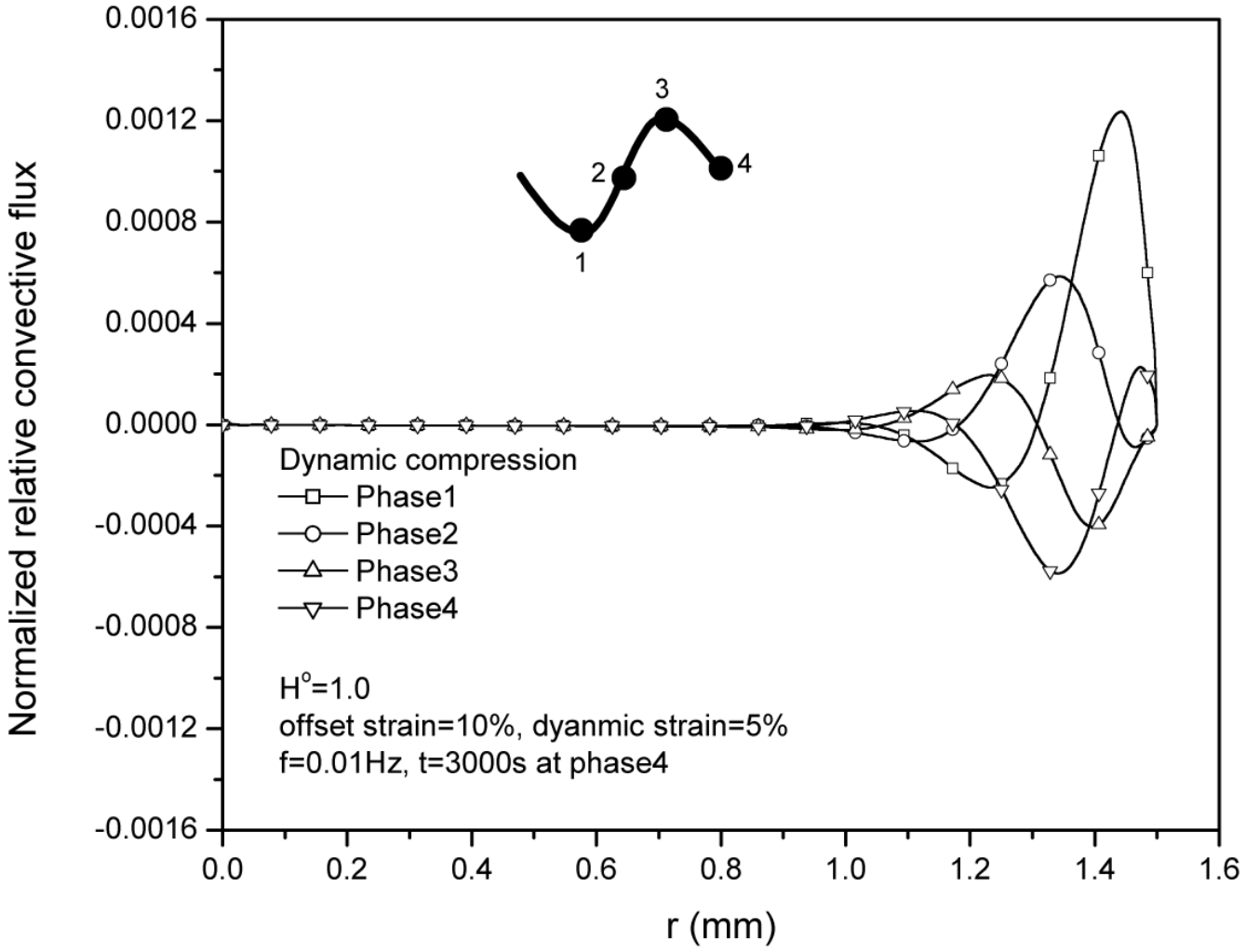

Figure 7.
Relative convective flux J^{o}_{RC} (normalized by $c^{o}_{i} H_A k_0/h$) distributions within the tissue during 30th cycle at 5% dynamic compression of 0.01Hz.

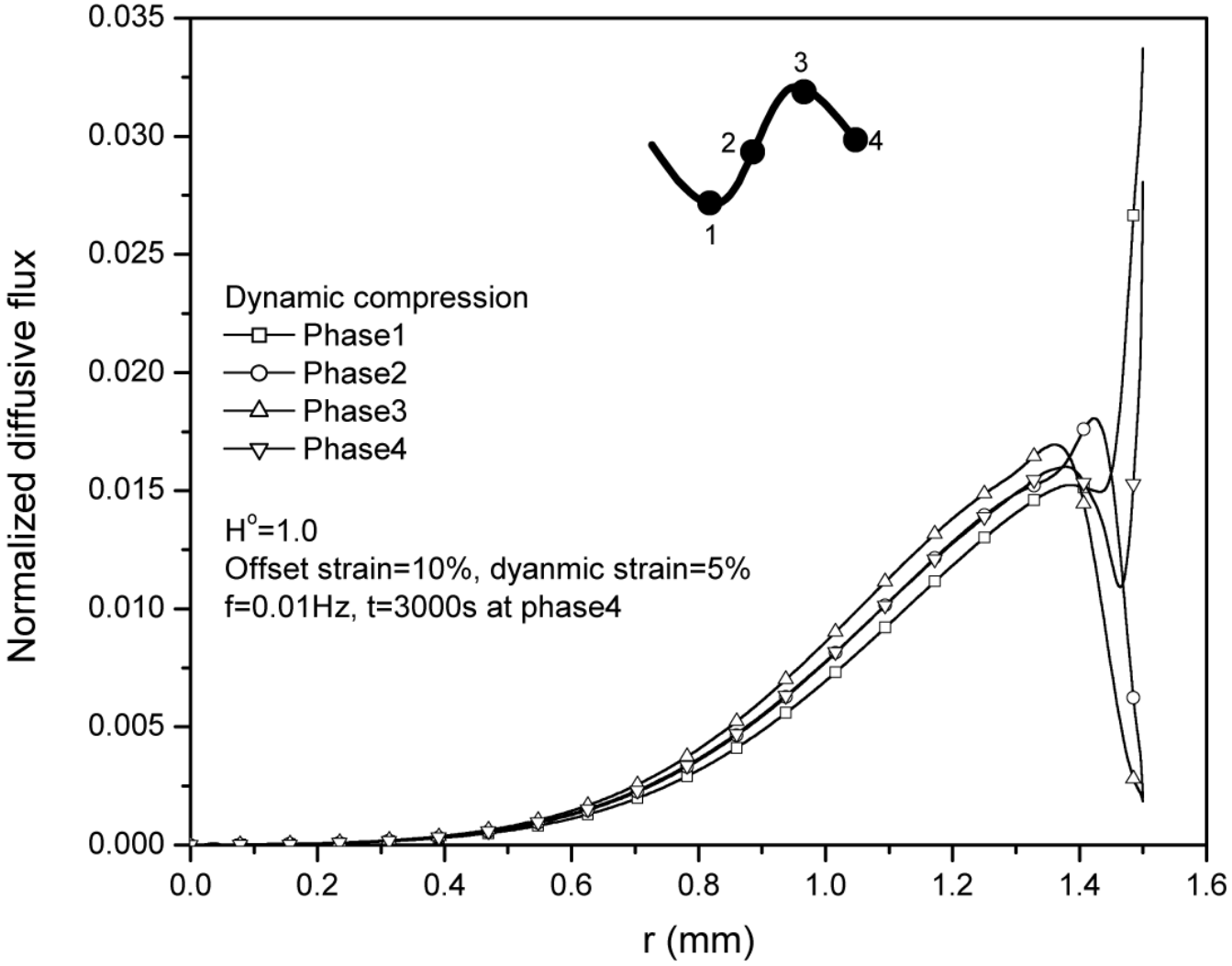

Figure 8.
Diffusive flux J^o_D (normalized by $c^o_i H_A k_0/h$) distributions in cartilage sample during 30th cycle at 5% dynamic compression of 0.01Hz.

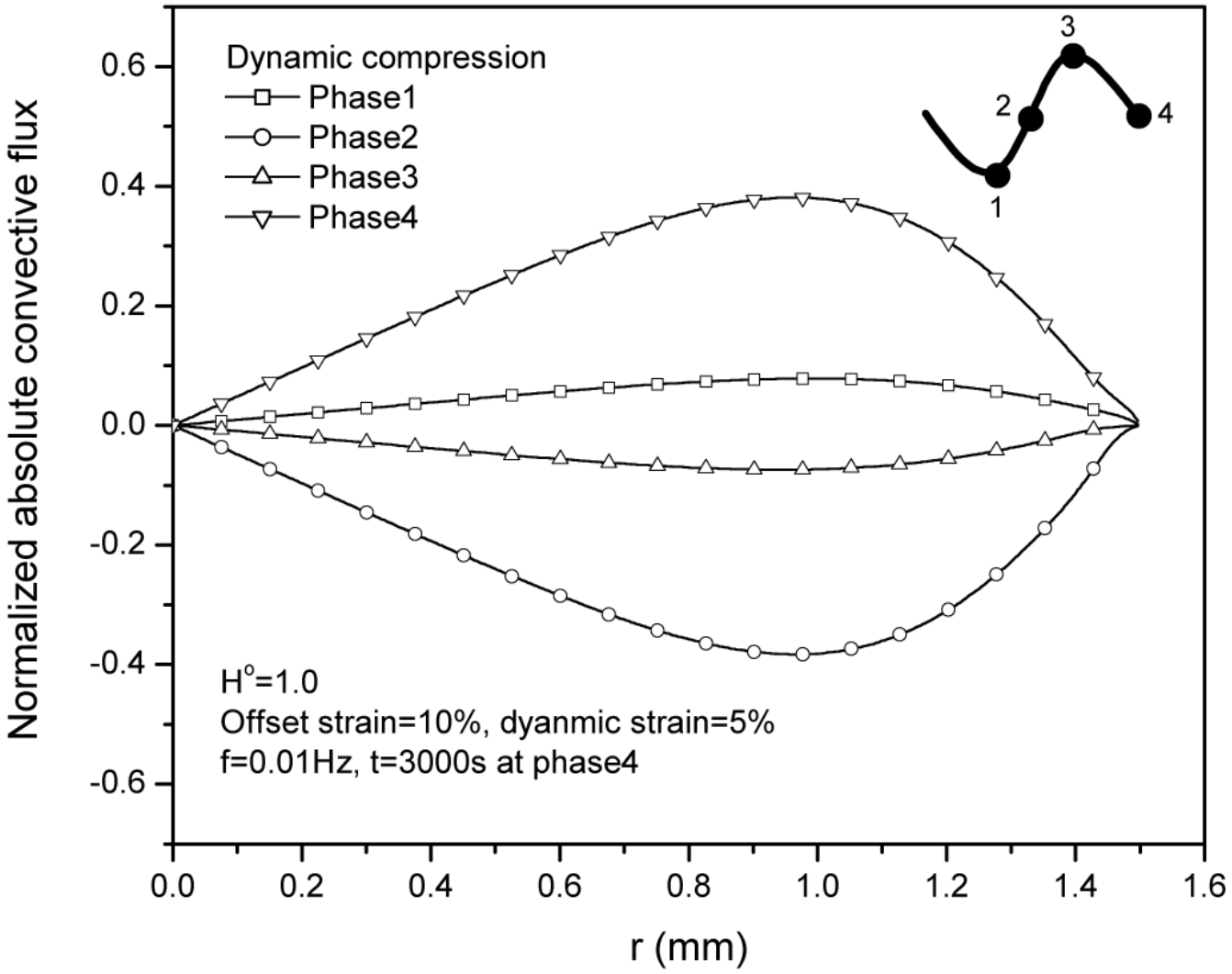

Figure 9.
Absolute convective flux J^o_{AC} (normalized by $c^o_i H_A k_0/h$) distributions within the tissue during 30th cycle at 5% dynamic compression of 0.01Hz.

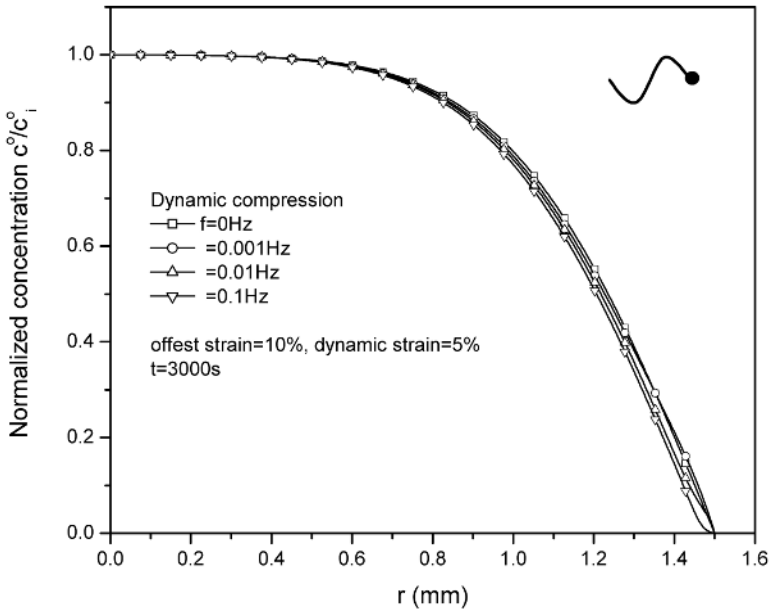

Figure 10.
Effect of loading frequency on solute concentration distributions within the tissue after 3000s desorption at 5% dynamic compression.

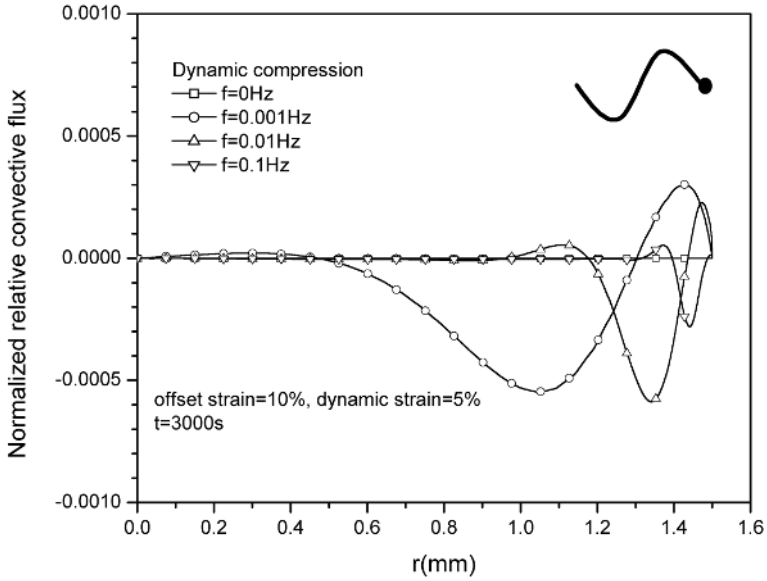

Figure 11.
Effect of loading frequency on the distributions of relative convective flux J^o_{RC} (normalized by $c^o_i H_A k_0/h$) within the tissue under 5% dynamic compression at t=3000s.

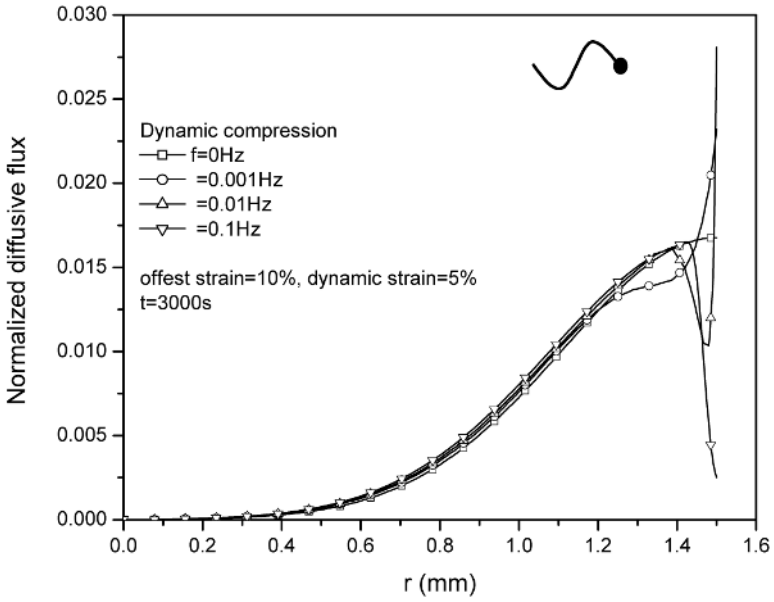

Figure 12.
Effect of loading frequency on the distributions of diffusive flux J^o_D (normalized by $c^o_i H_A k_0/h$) within the tissue under 5% dynamic compression at t=3000s.

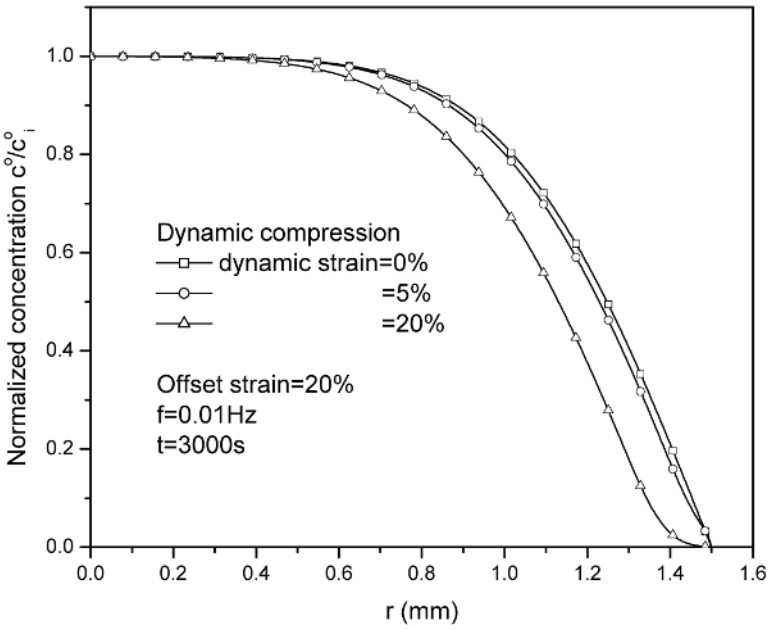

Figure 13.
Dynamic loading enhances solute desorption at a higher dynamic strain level (20%).